Beam Dynamics Simulation Tools of Insertion Devices at BESSY II *

J. Bahrdt, M. Scheer, G. Wüstefeld, BESSY, Berlin, Germany
e-mail of author: wuestefeld@bessy.de

Abstract

For beam dynamical simulations of insertion devices BESSY developed methods which are based on generating functions. These routines are symplectic and very fast. A summery of the work done on this subject is presented. Additionally, effects of end pole fields on beam dynamics are discussed, focused on the sextupole like field content of the insertion devices.

THE MACHINE OPTICS

BESSY II is a double bend, 16-cell, low emittance electron storage ring, see the layout in Fig.1 and the main parameters in Tab.1. Presently there are 15 insertion devices (ID) in operation, Tab. 2. The optics is designed in such a way, that strong superconducting insertion devices can be operated in the ring. Each second straight section of the ring is a low beta section, where strong IDs are placed, Fig.2. At these places the horizontal and vertical beta functions are focused to about 1 m. In this way, the optics distortion by strong IDs are kept small and the emittance is damped to about 70% of its original value. For beam injection the gaps of the IDs are opened, the fields of the superconducting IDs are not changed. Depending on the gap or field strength of the individual ID, a feed forward correction for residual orbit distortion (additionally to the regular orbit correction) and tune shift is set up.

TRACKING WITH GENERATING FUNCTIONS

For beam dynamics studies of the storage ring optics tracking calculations across IDs are required. The IDs are composed by 3-dimensional magnetic fields.

*Work supported by the Bundesministerium für Bildung, Wissenschaft, Forschung und Technologie and by the Land Berlin.

Table 1: BESSY II storage ring parameters

nom. energy	1.7 GeV
nat. emittance	5.5 nmrad
circumference	240 m
rf-frequency	500 MHz
typ. inject. current	250 mA
nat. chromaticity ξ_x, ξ_y	-52, -26
long. damping time	8ms

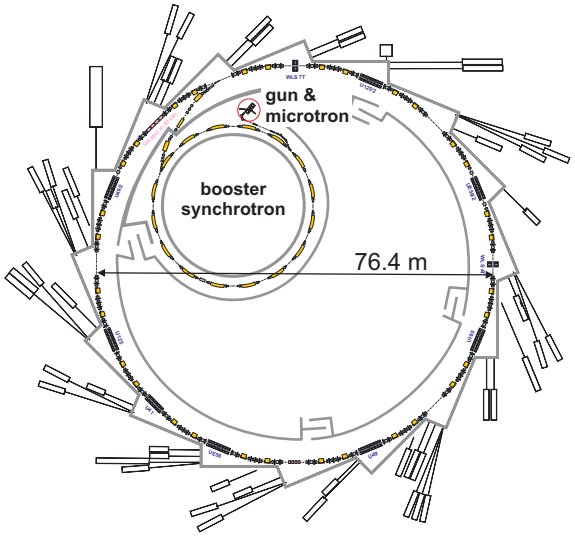

Figure 1: Layout of the BESSY II storage ring

It would not be sufficient to model them with the usual 2-dimensional magnetic multipoles, where standard mapping routines are available. For the mapping one would like to have a routine, that transforms a given set of initial, transverse particle coordinates to a set of final coordinates over a specified longitudinal section. Different to more common integration methods, which are based on 'infinitesimal' short integration steps, BESSY developed several types of ID tracking routines based on generating functions (GF). Most of this work is published in the proceedings of

Table 2: Insertion device parameters (U=planar ID, UE=helical ID, sc=superconducting ID, WLS=wavelength shifter, mPW=multipole wiggler, *= vertical tune shift)

name	devices	length	B_{max}-field
U-139	1	1.39 m	1.47 T
U-125	2	3.87 m	1.36 T
U-49	2	4.10 m	0.80 T
U-41	1	3.25 m	0.66 T
UE-56	2	3.36 m	0.77 T
UE-52	1	4.00 m	0.74 T
UE-49	1	3.09 m	0.71 T
UE-46	1	3.24 m	0.68 T
sc-WLS	1	0.008*	4(6) T
sc-WLS	2	0.02*	6.8 T
sc-MPW	1	0.075*	7 T

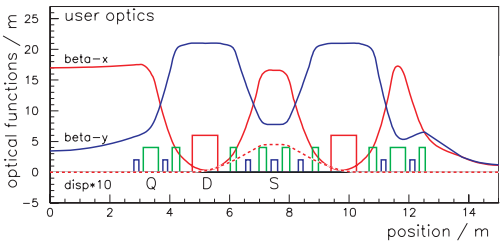

Figure 2: The BESSY II machine optics with its high and low beta straights. Q,D,S indicate types of quadrupoles, dipoles and sextupoles, respectively.

the PAC and EPAC, in this note a summary of this work is presented. [1]

The advantage of the GF is, that these methods are principally valid and fully symplectic for finite step lengths. A larger part of an ID or even the complete ID can be taken in a single step. This makes these routines very fast, as long as the transformation becomes not too nonlinear. One has no information on the particle position in between the steps, but this is acceptable for most of the tracking situations, where one is not interested in the particle positions inside the device. However, to achieve the GF is a more complicated way, as is shown in the next sections. The physics behind the GF is based on the Hamiltonian mechanics and can be found in text books, such as [2]. We present a short recipe, how this method is set up and applied. A comparison of the computing speed and accuracy of these routines is given in [3].

Numerical Generating Function

The first method discussed will be the numerical GF [4], [5]. This approach is very well suited for strong, superconducting devices. The magnetic field of these devices can be derived from a 3-dimensional magnet code or from magnetic field measurements. If only 2-dimensional parts of the field are known, it has to be completed to a 3-dimensional field. This can be done by a Fourier like expansion of the scalar potential V by harmonics of the type

$$V = -\sum (B_0/k_{yi}) \cos(k_{xi}x) \sinh(k_{yi}y) \cos(k_{zi}z), \quad (1)$$

where for the wave numbers the relation $k_{xi}^2 + k_{zi}^2 = k_{yi}^2$ holds. The coordinates are taken from a Cartesian system, where x, y and z are the horizontal, vertical and longitudinal axes, respectively. The field expansion by ('Halbach') harmonics satisfies the Maxwell equations.

An integration routine is used to track about 1000 particle orbits across the device. The orbits are selected in a range which covers the expected dynamic aperture. The result will be a set of initial, transverse particle coordinates $(x_i, y_i, p_{xi}, p_{yi})$ taken at the longitudinal position z_i and a set of final coordinates $(X_f, Y_f, P_{xf}, P_{yf})$ taken at Z_f. The coordinates are described by position (Cartesian system) and canonical momenta. The relation between the slope of the trajectory (X', Y') and the canonial momenta is given by $P_x = \tilde{A}_x + X'/\sqrt{1 + X'^2 + Y'^2}$ and $P_y = \tilde{A}_y + Y'/\sqrt{1 + X'^2 + Y'^2}$. For the vector potential (A_x, A_y, A_z) a scaling by the magnetic rigidity $B\rho$ is applied and we will use the abbreviation $(\tilde{A}_x = A_x/B\rho, \tilde{A}_y = A_y/B\rho, \tilde{A}_z = A_z/B\rho)$. One could imagine to perform a polynomial fit to the resulting coordinates, which maps the initial values to the final ones in a single step, but this would lead to a non-symplectic result. The method of the numerical GF does apply this idea, but transform it into a symplectic mapping routine.

The set of coordinates is separated into two, disjunctive chosen subsets. Each one contains half of the initial coordinates and half of the final coordinates. Details of this splitting depend on the type of GF which is used. There are four types common, let us take the GF named F_2. This function F_2 depends on the initial position and the final momentum coordinates, $F_2 = F_2(x_i, y_i, P_{xf}, P_{yf})$. A different type of GF would depend on a different subset of coordinates. It is a unique property of the GF that the complementary subset of coordinates can be derived from the GF by the following relations,

$$\begin{aligned} X_f &= \partial F_2/\partial P_{xf}, \quad & p_{xi} &= \partial F_2/\partial x_i, \\ Y_f &= \partial F_2/\partial P_{yf}, \quad & p_{yi} &= \partial F_2/\partial y_i. \end{aligned} \quad (2)$$

The GF itself needs still to be constructed in an appropriate way.

There is some freedom in setting up the explicit form of the GF. In case of the numerical GF we chose a polynomial fit of the type

$$F_2(x_i, y_i, P_{xf}, P_{yf}) = \sum_{k+l+m+n}^{M} a_{klmn} x_i^k y_i^l P_{xf}^m P_{yf}^n. \quad (3)$$

The coefficients a_{klmn} can be fitted by the complete set of coordinates and by the equations (2).

By taking a 2nd order expansion (M=2) of F_2 and applying equs. (2), a linearly coupled equation system of the coordinates is obtained, which can be solved for the linear transfer matrix. This would be sufficient to model the quadrupole focusing effects of the ID, but one would like to have at least octupole terms included. Therefore, we take M=4 or M=6 for the fit as a good compromise, where M=4 starts to model octupole like effects. About 60 coefficients a_{klmn} are required, if symmetry properties of the ID are included, such as midplane and reflection symmetry.

The implicit coordinate relations derived from F_2 are solved by a Newton fit routine. The resulting

[1] Our first paper on this subject was published 1984 [1], where this method was applied for beam dynamics studies in FFAG accelerators.

mapping routine is symplectic, independent how accurate the polynomial coefficients a_{klmn} are derived. Once the routine is set up, it is extremely fast. For each superconducting ID we tailor a GF describing its mapping properties. These IDs are typically strong focusing devices of minor nonlinear properties. The 3-dimensional, harmonic field expansion and the calculation of the numerical GF is part of the program package 'WAVE' [6]. The numerical GF can be applied to a varity of fields, as long as the transformation becomes not too nonlinear.

Analytical Generating Function

The second method is based on a Taylor expanded, analytical GF [7], [8],[9],[10]. We consider a mapping from the longitudinal position z_i to Z_f, positions in between are written in capital letters and without index i or f. We assume, that the vector potential can be expressed analytically by not too complicated functions. Complicated potential expressions will limit this method. This can be inserted into the Hamilton-Jacobi-Equation (HJE) [2],

$$H(X, Y, P_x, P_y) + \partial F/\partial Z = 0, \tag{4}$$

where H is the Hamiltonian function. The Hamiltonian of a charge in the magnetic field, expanded to second order is given by

$$H = (P_x - \tilde{A_x})^2/2 + (P_y - \tilde{A_y})^2/2 - \tilde{A_z}. \tag{5}$$

For the GF we select again F_2.

The coordinate transformation as described by the HJE is of special character. It is a kind of backward transformation, from the particle coordinates (X, Y, P_x, P_y) at position Z to the initial position z_i. One needs to distinguish between initial (index i) and final (index f) coordinates and between 'new' and 'old' coordinates. The HJE describes the transformation from the old, Z-dependent position to the new, constant position which is the initial one. The Hamiltonian of the old coordinates is explicitly given in the HJE, the Hamiltonian of the new (constant) coordinates is zero. The GF connects the new and the old coordinates in a mixed way as discussed above. The new particle coordinates of the transformation are our initial coordinates $(x_i, y_i, p_{xi}, p_{yi})$, the old ones will finally become our coordinates $(X_f, Y_f, P_{xf}, P_{yf})$ if Z is approaching Z_f.

As in the numerical case, the GF of type F_2 depends on the mixed coordinates, old position coordinates (no index) and new momenta (index i), $F_2 = F_2(X, Y, p_{xi}, p_{yi})$. The momenta P_x, P_y in the Hamiltonian can be expressed by F_2, and the HJE becomes

$$\begin{aligned}&(\partial F_2/\partial X - \tilde{A_x})^2/2 + (\partial F_2/\partial Y - \tilde{A_y})^2/2 \\ &-\tilde{A_z} + \partial F_2/\partial Z = 0\ .\end{aligned} \tag{6}$$

The resulting HJE is an equation, which is of first order in three different partial derivatives of F_2. To solve this equation for F_2 we choose as an Ansatz a series expansion of the type

$$F_2 = \sum_{l,m,n} f_{lmn} p_{xi}^l p_{yi}^m x_3^n, \tag{7}$$

where the coefficient f_{lmn} are dependent on the position coordinates (X, Y, Z). The f_{lmn} are calculated by a recursion approach. The recursion is started with a drift transformation,

$$F_2^{drift} = X p_{xi} + Y p_{yi} - Z(p_{xi}^2 + p_{yi}^2)/2. \tag{8}$$

The required longitudinal integration of the coefficients is performed over the full range of Z, from z_i to Z_f.

The variable x_3 can be chosen as $x_3 = 1/B\rho$, the common scaling factor of the vector potential. But in most cases, there are more common factors in the vector potential components, which can be included into x_3. The special choice of $x_3 \sim 1/B\rho$ allows us to solve the differential equation by a recursion formula. This is done with a short REDUCE [11] routine, see appendix. The expansion order is limited by the increasing size of the f_{lmn} terms and by the expansion order of the Hamiltonian of equ.(5). A 4th order expansion would require an improoved Hamiltonian. We could not find a recursion formula, based on the expansion with respect to the four coordinates (X, Y, P_x, P_y).

As an example the general solution in 2nd order, where the vector potential is replaced as far as possible by magnetic field expressions, is given by,

$$\begin{aligned}
f_{001} &= \int A_z dZ \\
f_{002} &= -\int((\int B_y dZ)^2 + (\int B_x dZ)^2) dZ/2 \\
f_{101} &= \int\int B_y dZ dZ \\
f_{011} &= -\int\int B_x dZ dZ \\
f_{100} &= X_f, \qquad f_{200} = -Z_f/2, \\
f_{010} &= Y_f, \qquad f_{020} = -Z_f/2.
\end{aligned} \tag{9}$$

The double integration of a function $g = g(Z)$ has to be performed like

$$\int\int g dZ dZ = \int_{z_i}^{Z_f} \int_{z_i}^{Z} g(Z') dZ' dZ. \tag{10}$$

Beside the f_{001} term, this result is independent on the choice of the vector potential. The f_{001} term is used to calculate the momentum. When the canonical momentum is turned into the orbit slope (X', Y') the vector potential is required and together with the A_z term the result becomes independent on the explicit choice of the vector potential, for example, in lowest order

$$\begin{aligned}
X' &= P_{xf} - \tilde{A_x} = \partial F_2/\partial X_f - \int(\partial \tilde{A_x}/\partial Z) dZ \\
&= x_3 \partial f_{001}/\partial X_f - \int(\partial \tilde{A_x}/\partial Z) dZ + ... \\
&= \int(\partial \tilde{A_z}/\partial X_f - \partial \tilde{A_x}/\partial Z) dZ + ... \\
&= -\int B_y/B\rho dZ + ...
\end{aligned}$$

The leading order for X' and the term f_{101} are named the first and second field integrals of an ID (similar for the B_x field, see next chapter on end pole effects).

The general, 3rd order solution of F_2 together with the explicit, device specific vector potential are used to set up the FORTRAN routines. It solves the implicit equations (2) of the coordinates. They could also be solved analytically by two second order equations in the momenta, but a Newton fit routine seems to be faster and of higher accuracy. The integrated f_{lmn} terms become simplified in case of the periodic character of the longitudinal fields of the IDs, it averages over oscillating terms. Once the FORTRAN routine for a generic type of ID is set up, it can be used for all devices of this type. One only needs to pass the characteristic parameters to the routine, such as the 3 wave numbers k_x, k_y, k_z, max. field strength in the midplane, number of periods and particle energy in case of a planar device as discussed below.

As an example, the GF of the planar device expanded to 3rd order is given [9] with the leading term of the scalar potential of eqn. (1). The result is expressed as

$$\begin{aligned} F = \quad & F_{00} + F_{10}p_{xi} + F_{01}p_{yi} + F_{20}p_{xi}^2 \\ & + F_{11}p_{xi}p_{yi} + F_{02}p_{yi}^2, \end{aligned} \tag{11}$$

where the expansion with respect to x_3 is included into the F_{ij}-coefficients, $F_{ij} = f_{ij0} + f_{ij1}x_3 + f_{ij2}x_3^2 + f_{ij3}x_3^3$, with $f_{ijk} = 0$ for $i + j + k > 3$. In this example the variable x_3 is chosen as $= 1/(k_z\rho_{min})$, where ρ_{min} is the minimal orbit curvature in the midplane of the ID. Typical values of k_z are 60 1/m and of ρ_{min} =5 m, yielding $x_3 = 1/300$ or even smaller. Depending on the device strength and period length, the mapping can be taken over n multiple integers of the longitudinal period length λ_z, $Z_f = n\lambda_z$.

By applying the abbreviation $c_x = \cos(k_x X_f)$, $s_x = \sin(k_x X_f)$, $c_y = \cosh(k_y Y_f)$ and $s_y = \sinh(k_y Y_f)$ the F_{ij}-coefficients are given as,

$$\begin{aligned} F_{00} = \quad & -Z_f x_3^2((k_y c_x c_y)^2 + (k_x s_x s_y)^2)/(2k_y)^2 \\ & + Z_f x_3^3 s_x c_y k_x((k_x s_y)^2 - (k_y c_x)^2)/(2k_y^2 k) \\ F_{10} = \quad & X_f - Z_f^2 x_3^2 k_x s_x c_x((k_z c_y)^2 + k_x^2)/(2k_y)^2 \\ F_{01} = \quad & Y_f + Z_f^2 x_3^2 k_y s_y c_y((k_z c_x)^2 + k_x^2)/(2k_y)^2 \\ F_{11} = \quad & -Z_f x_3 s_y c_x (k_y^2 + k_x^2)/(k_z k_y) \\ F_{20} = \quad & -Z_f/2 + Z_f x_3 k_x c_y s_x/k_z \\ F_{02} = \quad & -Z_f/2 - Z_f x_3 k_x c_y s_x/k_z. \end{aligned} \tag{12}$$

This result can be used, to derive an approximated Hamiltonian of the transformation. Because the integration was performed over multiples of the longitudinal period, the result will be an averaged Hamiltonian, not including oscillating terms. The Hamiltonian is derived from the HJE, $H = -\partial F_2/\partial Z$, where F_2 is taken from the expanded solution. For simplicity, we take for F_2 only a drift transformation plus the F_{00} term (2nd order in p_{xi}, p_{yi}, x_3),

$$F_2 = f_{002}x_3^2 + Xp_{xi} + Yp_{yi} - Z(p_{xi}^2 + p_{yi}^2)/2. \tag{13}$$

The mixed coordinates have to be replaced by coordinates taken at position Z. Therefore, we calculate $P_x = \partial F_2/\partial X = p_{xi} + ...$ in first order and similar for P_y. The leading terms of the averaged Hamiltonian are

$$\begin{aligned} H = \quad & (P_x^2 + P_y^2)/2 + ((k_y c_x c_y)^2 \\ & + (k_x s_x s_y)^2)/(2k_y k_z \rho_{min})^2, \end{aligned} \tag{14}$$

in agreement with the Hamiltonian derived in the note [12] by L. Smith. The leading 3-dim multipole content integrated over one period can be derived from the expension of this Hamiltonian to 4th order,

$$\begin{aligned} H = \quad & (P_x^2 + P_y^2)/2 + (1 + (k_y Y)^2 + (k_x X)^2 \\ & + (k_y Y)^4/3 - (k_y k_x Y X)^2 + (k_x X)^4/3) \\ & /(2k_z\rho_{min})^2 \end{aligned} \tag{15}$$

yielding the quadrupole strenth from the 2nd order terms and the octupole strength form the 4th order terms.

A second FORTRAN routine was set up to simulate helical insertion devices of the APPLE II type [13]. For this an analytical representation of the field is required, which can be derived from the scalar potential, $V = B_0(V_1 + V_2 + V_3 + V_4)/8$, with

$$\begin{aligned} V_1 &= +(e^{+k_y y}c_{x-}/k_y + e^{+k_z y}/k_z)c_{z+} \\ V_2 &= +(e^{+k_y y}c_{x+}/k_y + e^{+k_z y}/k_z)c_{z-} \\ V_3 &= -(e^{-k_y y}c_{x+}/k_y + e^{-k_z y}/k_z)c_{z+} \\ V_4 &= -(e^{-k_y y}c_{x-}/k_y + e^{-k_z y}/k_z)c_{z-}, \end{aligned} \tag{16}$$

where, $c_{x\pm} = \cos(k_x(x \pm x_0))$ and $c_{z\pm} = \cos(k_z z \pm \psi/2))$. The individual helical ID is characterized by the parameters B_0, x_0, k_x, k_y, k_z, shift parameter ψ and the number of periods. The helical potential is an example of a more complicated field, which can be handled with the analytical GF expansion.

END POLE EFFECTS

The end poles consist of only a few poles of the whole ID, but these poles have to provide special tasks. They guide the closed orbit from the outside of the ID to the periodic closed orbit inside of the ID and back to the outside. This is properly done, if the first and second field integral I_1, I_2 are zero,

$$\int_{-L}^{+L} B_y dz = 0, \quad \int_{-L}^{+L}\int_{-L}^{z} B_y dz' dz = 0, \tag{17}$$

and similar for the B_x-field. A single pole could give a strong kick to the beam, but the overall effect is small, if the condition of the field integrals are satisfied. The first integral states, that the average field should be zero to avoid a transverse kick to the transferred beam. The second integral poses constrains on the

distribution of the field, to avoid a transverse shift of the beam. The conditions of equ. (17), if violated, can have a strong impact on the nonlinear dynamics of the beam. This is discussed in this chapter and shown for the example of the sextupole content of the ID poles, [13].

A typical ID pole introduces a strong sextupole-like field to the beam optics. If the ID poles are strictly periodical and alternating in sign, their strength averaged over two adjacent poles vanishes. The end poles, in general, are different to the periodic part of the ID. From the potential function of the field, terms which characterize sextupole like fields can be derived (at x=y=0):

$$\begin{array}{ll} \partial^3 V/\partial x^3, & \partial^3 V/\partial x^2 \partial y, \\ \partial^3 V/\partial x \partial y^2 & \partial^3 V/\partial y^3. \end{array} \qquad (18)$$

In case of a polynomial expansion, these fields increase with the transverse position coordinate in the same order as the two-dimensional sextupole fields. Because of the 3-dimensional character of the ID fields there are 4 terms, compared with two expressions (skew and normal) in the two-dimensional case. For the ID one expects an oscillation of the strength of these terms along the beam axis with an average value of zero. The amplitude of these oscillations could be large, for example the term $\partial^3 V/\partial y^3$ integrated over half a period could yield as much as 80 T/m for a typical helical ID of the BESSY ring. For comparison, the correction sextupoles of the BESSY II optics reach values of 50 T/m. With respect to these fields the ID can be considered as an alternating series of strong sextupole kicks.

To find out the conditions, that the effects of the sextupole fields on the beam is small, Collins 'distortion functions' [14] will be applied. These functions describe the deformation of the beam envelope by sextupole fields. Instead of 5 distortion functions for normal two-dimensional sextupoles there are now 7 in case of an ID without skew terms. If only a single sextupole-like kick as a source of distortion is considered, then the distortion functions B_i (i=1-7) become very simple, they are all of the type:

$$B_i = \frac{1}{2} s_i(z) \cos(\delta_i + \phi_{i0} - \phi_i) / \sin(\phi_{i0}), \qquad (19)$$

were the phase around the ring is $2\phi_{i0}$ and B_i is evaluated outside the ID at ϕ_i. The longitudinal position z and the phases are defined in such a way that $z = \phi_i = \delta_i = 0$ at the starting (or reference) point. All phases are scaled, dependent on the type i of the distortion function. There are 4 different δ_i-scalings:

$$\begin{array}{ll} \delta_{1,5} = \tilde{\varphi_x}, & \delta_2 = 3\tilde{\varphi_x}, \\ \delta_{3,6} = 2\tilde{\varphi_y} + \tilde{\varphi_x}, & \delta_{4,7} = 2\tilde{\varphi_y} - \tilde{\varphi_x}, \end{array} \qquad (20)$$

and similar relations for skew terms (exchange x and y). $\tilde{\varphi_x}$ and $\tilde{\varphi_y}$ are the unscaled horizontal and vertical betatron oscillation phases. Similar relations are valid for ϕ_i and ϕ_{i0}. Also the sextupole kicks are scaled. The strength of the kick is integrated over one pole (for example, $\int \partial^3 V/\partial^2 x \partial y dz = \Delta z V_{yxx}$), and multiplied by scaling factors depending on the local beta functions:

$$\begin{array}{lcl} s_{1,2}(z) & = & \frac{1}{3}\Delta z V_{yxx} \beta_x \sqrt{\beta_x} \\ s_{3,4}(z) & = & \frac{1}{6}\Delta z V_{yyy} \beta_x \sqrt{\beta_y} \\ s_{5,6,7}(z) & = & \frac{1}{3}\Delta z V_{yxx} \beta_y \sqrt{\beta_x} \end{array} \qquad (21)$$

For the evaluation of a special B_i, sextupole kicks and phase functions with equal indices have to be combined.

The distortion function B_i of equ. (19) can be decomposed into a $\cos(\phi_i - \phi_{i0})$- and a $\sin(\phi_i - \phi_{i0})$-wave. The amplitudes A_c and A_s of these waves for an extended source $s_i(z)$ like the ID are proportional to the integrals

$$\begin{array}{l} A_c \propto \int_{ID} s_i(z) \cos\delta_i dz \quad \text{and} \\ A_s \propto \int_{ID} s_i(z) \sin\delta_i dz. \end{array} \qquad (22)$$

One would like to have these amplitudes equal to zero to minimize optics distortions. If the phase advance over the ID is small, $\sin\delta_i$ is proportional to z and $s_i(z)$ can be replaced by the unscaled sextupole strength $s(z) = V_{yyy}$, V_{yyx}, V_{yxx} and V_{xxx}, respectively, regarding the beta functions as constant. The condition for vanishing amplitudes A_c and A_s can be further simplified by applying partial integration:

$$\begin{array}{l} A_c \approx \int_{-L}^{L} s(z) dz \equiv 0, \\ A_s \approx \int_{-L}^{L} \int_{-L}^{z} s(z') dz' dz \equiv 0, \end{array} \qquad (23)$$

yielding a similar presentation as for the I_1 and I_2 integrals of equ. (17). In case of a $\cos(k_z z)$-dependency of the ID-fields, both, the field integrals I_1, I_2 and the integrals A_c, A_s are naturally matched, which is not the case if the ID starts with a more $\sin(k_z z)$-dependency. IDs with a more complicated field distribution like helical IDs should be carefully matched.

Figs. 3 and 4 show simulations with a helical ID, described by the potential function of equ. (16). In Fig. 3 the distortion function of type B_i for i=1 is shown. In this case all scaled phases can be replaced by the appropriate horizontal betatron oscillation phase. The distortion generated by the sextupole like kicks of the ID is plotted over one lattice cell. The dashed line shows the situation if no end poles are applied. The distortion is large and spreads out all over the cell. The red line in Fig. 3 shows the same configuration but with matched end poles, it is clearly seen that the distortion is nearly perfectly enclosed in the ID, like a closed sextupole bump.

These two situations are compared in Fig. 4 on the basis of tracking simulations of the vertical phase space. A particle is started in the straight section with

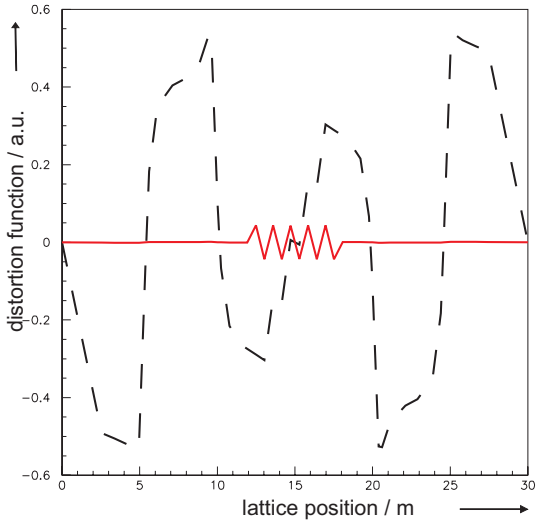

Figure 3: Distortion function B_1 for the matched (red) and unmatched case along a BESSY unit cell. The simulation was performed for sextupole fileds introduced by one ID of 12 poles and no further sextupoles in the lattice.

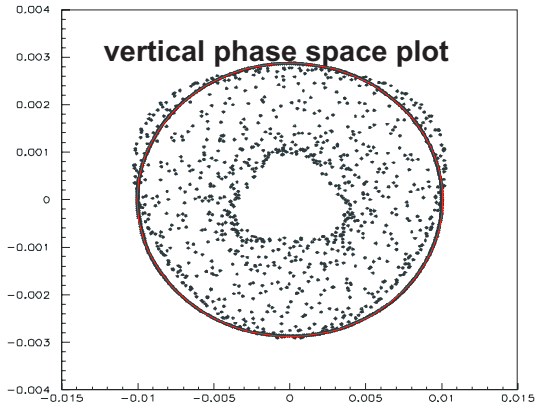

Figure 4: Vertical phase space plot for the matched (red) and unmatched case.

1 *cm* amplitude in both planes and tracked for 1000 turns. The unmatched case (dots) shows a large smear due to the sextupole fields of the ID. The effect of a good matching is clearly visible, the phase space figure shows nearly a perfect circle (red color). The matching is achieved by end poles on either side of the ID, each one composed by two half poles. The fields of the matching poles are derived from the potential V of equ. (16). At the entrance side for the first half pole the potential $+\frac{1}{4}V$ is applied, for the second half pole $-\frac{3}{4}V$ is used. At the exit side the sequence is reversed, using $+\frac{3}{4}V$ and $-\frac{1}{4}V$. Inside the periodic part of the ID the fields are derived from $\pm V$. Applying these end poles both, closed orbit and distortion functions, are well matched.

SUMMARY

The GF approach for beam dynamical simulation of ID effects is a fast and symplectic tool. It can be well applied to 3-dimensionals magnetic fields. Methods for a numerical routine and for an analytical routine are set up. To achieve good dynamic apertures the end poles of the IDs have to be designed to match properly the requirements of the field integrals.

REFERENCES

[1] H. Lustfeld, Ph. Meads, G. Wüstefeld et al., 'A Proper Canonical Algebraic Mapping Transformation', Proceedings of the 1984 Linear Accelerator Conference, GSI-84-11 Conf., Darmstadt (Germany) Sep. 1984.

[2] H. Goldstein, Klassische Mechanik, Akademische Verlagsgesellschaft, Frankfurt (Germany).

[3] M. Scheer, G. Wüstefeld, 'Tracking Routines for General Insertion Devices', Proceedings of the PAC 1997, Vancouver (Canada).

[4] M. Scheer, 'Effects of a Superconducting Wavelength Shifter on the Planned Storage Ring BESSY II, Part I: Canonical Tracking Calculations', BESSY Tech. Report, TB 169/92, BESSY, Berlin Germany.

[5] M. Scheer, G. Wüstefeld, 'Influence of a Wavelength Shifter on the Performance of the Synchrotron Light Source BESSY II', Proceedings of the EPAC 1992, Berlin (Germany).

[6] M. Scheer, 'WAVE', BESSY, Berlin (Germany)

[7] J. Bahrdt, G. Wüstefeld, 'A New Tracking Routine for Particles in Undulator and Wiggler Fields', Part I, II and III, BESSY TB Nr. 168 and TB Nr. 163, BESSY, Berlin (Germany), 1990.

[8] J. Bahrdt, G. Wüstefeld, 'A Taylor-Expanded Generating Function for Particle Motion in Arbitrary Magnetic Fields', Proceedings of the EPAC 1992, Berlin (Germany).

[9] J. Bahrdt, G. Wüstefeld, ' Canonical Particle Tracking in Undulator Fields', Proceedings of the PAC 1991, San Francisco (USA).

[10] G. Wüstefeld, 'Particle Tracking with Generating Functions of Magnetic Fringing Fields', Proceedings of the PAC 1995, Dallas (USA).

[11] A. C. Hearn, 'REDUCE'-Version 3.6, 1995, Santa Monica (USA).

[12] L. Smith, 'Effect of Wigglers and Undulators on Beam Dynamics', ESG Tech. Note-24, page 8, 1986.

[13] M. Scheer, G. Wüstefeld, 'Canonical Particle Tracking and End Pole Matching of Helical Insertion Devices ' Proceedings of the PAC 1997, Vancouver (Canada).

[14] T. L. Collins, 'Distortion Functions', Fermilab-84/114, 1984, FNAL, Batavia, IL 60510 USA

APPENDIX:
REDUCE-code for 3rd Order Generating Function of Planar ID

```
%definition of potential:
v:=-(b0/ky)*cos(kx*x)*sinh(ky*y)*cos(k*z);
ax:= -int(df(v,y),z) ;
ay:= int(df(v,x),z) ;
az:=0 ;

%definition of series:
operator f ;
f2:= 0 ;
ord := 3 ;
for ic:=1:ord do for ix:=0:ord do
for iy:=0:ord do for i3:=0:ord do
if ix+iy+i3=ic then
<< depend f(ix,iy,i3),X,Y,z ;
f2 := f2 +
f(ix,iy,i3)*pix**ix*piy**iy*x3**i3 >> ;

%initial values of the series:
f(1,0,0) := X ; f(2,0,0) := -z/2 ;
f(0,1,0) := Y ; f(0,2,0) := -z/2 ;

%limitation of terms:
for ix:=0:ord+1 do for iy:=0:ord+1 do
for i3:=0:ord+1 do if ix+iy+i3>ord then
let pix**ix*piy**iy*x3**i3 = 0 ;

%definition of Hamiltonian:
h:=(Pfx-x3*ax)**2/2+(Pfy-x3*ay)**2/2-x3*az;

%substitution of the momenta:
h:=sub(Pfx=df(f2,X),Pfy=df(f2,Y),h);

%Hamilton-Jacobi equation:
hj := h + df(f2,z) ;

%iterative solution:
for ic:=1:ord do for ix:=0:ord do
for iy:=0:ord do for i3:=0:ord do
if ix+iy+i3=ic then
<< term :=
coeffn(coeffn(coeffn(hj,pix,ix),piy,iy),x3,i3);
if term neq 0 then <<
sol1 := solve(term=0,df(f(ix,iy,i3),z)) ;
sol2 := rhs(part(sol1,1)) ;
sol3 := int(sol2,z) ;
f(ix,iy,i3) := sol3-sub(z=0,sol3) ;
write " f",ix,iy,i3,"= ",f(ix,iy,i3) ;
>> >> ;

%resulting generating function:
f2 ;
end;
```